Sensors & Actuators: B. Chemical 276 (2018) 48–56

Contents lists available at ScienceDirect

Sensors and Actuators B: Chemical

journal homepage: www.elsevier.com/locate/snb

Lateral flow aptamer assay integrated smartphone-based portable device for simultaneous detection of multiple targets using upconversion nanoparticles

Birui Jin[a,b,c], Yexin Yang[b,c], Rongyan He[b,c], Yong Il Park[d], Aeju Lee[e,f], Dan Bai[c,g], Fei Li[b,c], Tian Jian Lu[h,i], Feng Xu[b,c], Min Lin[b,c,*]

[a] State Key Laboratory for Mechanical Behavior of Materials, School of Materials Science and Engineering, Xi'an Jiaotong University, Xi'an, 7100C49, PR China
[b] The Key Laboratory of Biomedical Information Engineering of Ministry of Education, School of Life Science and Technology, Xi'an Jiaotong University, Xi'an, 710049, PR China
[c] Bioinspired Engineering & Biomechanics Center (BEBC), Xi'an Jiaotong University, Xi'an, 710049, PR China
[d] School of Chemical Engineering, Chonnam National University, Gwangju, 61186, Republic of Korea
[e] International Research Organization for Advance Science and Technology (IROAST), Kumamoto University, Kumamoto, 8608555, Japan
[f] Magnesium Research Center, Kumamoto University, Kumamoto, 8608555, Japan
[g] Department of Biochemistry and Molecular Biology, School of Medicine, Xi'an Jiaotong University, Xi'an, 710049, PR China
[h] MOE Key Laboratory for Multifunctional Materials and Structures, Xi'an Jiaotong University, Xi'an, 710049, PR China
[i] State Key Laboratory of Mechanics and Control of Mechanical Structures, Nanjing University of Aeronautics and Astronautics, Nanjing, 210016, PR China

ARTICLE INFO

Keywords:
Multiplexed detection
Lateral flow assay
Paper microfluidics
Point of care testing
Chemical antibody

ABSTRACT

Simultaneous detection of multiple targets with different analyte-recognition reactions in the same sample in a rapid, low-cost and reliable way has immense potential with widespread applications in food safety, medical diagnostics and environmental monitoring. Herein, we developed a lateral flow aptamer assay (LFAA) integrated smartphone-based portable device for highly sensitive and precise detection of multiple targets, using aptamers functionalized multi-colored upconversion nanoparticles as probes. The developed LFAA can provide rapid and sensitive analysis of three different kinds of targets (*i.e.*, small molecules, ions and bacteria) without significant cross-reaction by using separate color channels. By using the competitive format, the concentration of each target can be determined from the color intensity of the corresponding colored band. With the LFAA, we have achieved detection ranges of 10–10^4 ppb, 0.01–50 μg/mL and 150–2000 CFU/mL and detection limits of 5 ppb, 3 ng/mL and 85 CFU/mL for mercury ions, ochratoxin A and *Salmonella* (as template analytes), respectively. The LFAA was further used for detection in real water samples (*i.e.*, tap water) within 30 min. Subsequently, a smartphone-based device was used instead of a CCD camera to read the results, which could make the detection process rapid and portable. Therefore, the developed LFAA holds great potential as a sensitive, specific, convenient and stable platform for point-of-care detection of multiple targets in various fields.

1. Introduction

Multiple target testing (*i.e.,* the simultaneous detection of different types of targets in a single specimen) has recently gained significantly increased attention in the areas of environmental monitoring, medical diagnostics and food safety. For instance, pathogens, heavy metal ions and other toxic substances are all important indicators for water quality evaluation [1–3]. Also, clinical doctors often need to assess the content of bacteria, fungal specimens or toxins in blood samples simultaneously to precisely diagnose whether a symptom is caused by inflammation, fungal infection or toxin accumulation [4]. In addition, a worldwide public health issue, foodborne disease, is caused by different types of contaminants (*e.g.*, bacteria, antibiotics, illegal additives and pesticide residues) in food samples, which impacts almost 1 in 10 of the global population [5,6]. Therefore, it is of great importance to simultaneously detect of multiple targets in the same sample in a rapid, reliable and low-cost way.

The biggest challenge with existing analytical methods is that they are not sensitive, rapid, low-cost or capable of multiple targets detection at the same time. For example, polymerase chain reaction (PCR), liquid and gas chromatography and mass spectroscopy are known as the gold standard for analyzing samples and are capable of multiple target

* Corresponding author at: The Key Laboratory of Biomedical Information Engineering of Ministry of Education, School of Life Science and Technology, Xi'an Jiaotong University, Xi'an 710049, PR China.
E-mail address: minlin@mail.xjtu.edu.cn (M. Lin).

https://doi.org/10.1016/j.snb.2018.08.074
Received 2 May 2018; Received in revised form 13 August 2018; Accepted 15 August 2018
Available online 17 August 2018

Table 1
The sequences of the aptamer and the complementary DNA.

Sample Name	Sequence (5–3′)	Source
Aptamer 1 (OTA)	GCTGAGTCTGAGTCG ATCGGGTGTGGGTGGCGTAAAGGGAGCATCGGACA	Cruz-Aguado, J. A and Penner, G [26]
complementary DNA 1	CGCCACCCACACCCGAT	
Aptamer 2 (SE)	GCTGAGTCTGAGTCG TATGGCGGCGTCACCCGACGGGGACTTGACATTATGACAG	Xiaoyuan Ma et.al [27]
complementary DNA 2	CTGTCATAATGTCAAG	
Aptamer 3 (Hg^{2+})	GCTGAGTCTGAGTCG TCATGTTTGTTTGTTGGCCCCCCTTCTTTCTTA	Qing Li et.al [28]
complementary DNA 3	AAACAAACATGA	
complementary DNA of control part	CGACTCAGACTCAGC	

detection with high sensitivity and selectivity. However, these methods are expensive, time-consuming and require well-trained operators [7]. Paper-based lateral flow assays (LFAs) show great potential for point-of-care testing (POCT) due to their short turnaround time, sensitivity, specificity, robustness and cost-effectiveness [8]. However, lateral flow immunoassays (LFIAs), for example, are often developed for detection of a single target per assay [9,10]. Thus, several LFIA formats have been developed to address the challenge of detecting more than one analyte in a single strip, which lends to further opportunity to increase speed and decrease cost by screening multiple targets simultaneously [11–14]. However, these LFAs are associated with limitation of non-specific binding and crossover reactions, which can lead to false positive results [15]. Moreover, the inability to detect multiple targets based on different analyte-recognition reactions (*e.g.*, antibody-antigen reaction, complementary base pairing and dry chemical reaction) has greatly hindered its practical applications, since the recognition of multiple targets (*e.g.*, metal ions, food additives and pesticide residues) often require different analyte-recognition reactions. For instance, target capture based on antibody-antigen reaction is greatly compromised by the difficulty to raise antibodies for toxicants or non-immunogens (*e.g.*, metal ions, food additives and pesticide residues). Thus, it remains a big challenge to design LFAs capable of detecting multiple targets with different analyte-recognition reactions.

Aptamers, single-stranded DNA or RNA, are considered “chemical antibodies” due to their sequence-specific, target-binding functionality, which provides them a high affinity to form higher-order structures [16]. More importantly, the conformational diversity of aptamers makes them capable of recognizing a wider range of targets, such as amino acids, metal ions, polysaccharides, protein complexes, virus particles, bacteria and even whole cells, through hydrogen bonding, electrostatic interactions, shape effect, aromatic rings, and/or base pairing [17–21]. In addition, the synthetic feasibility of aptamers makes them easy to modify and tag, providing extraordinary flexibility in the development of POCT assays [21]. Thus, modified aptamers have been tethered to colorimetric particles (*e.g.*, gold nanoparticles) and then employed in lateral flow aptamer assays (LFAAs). Various types of LFAAs have been used to detect different targets, *e.g.*, sandwich format [22], competitive format [23], signal amplification for aptamer hybridization-based LFIAs [24] and other formats of LFAAs [25]. However, these existing colorimetric-based LFAAs suffer from poor detection limits and mainly aim at single target detection.

The use of fluorescence nanoparticles can significantly improve the detection limit (by one or two orders of magnitude), which satisfies various detection applications [10,14]. Upconversion nanoparticles (UCNPs) can convert near-infrared (NIR) excitation into visible emissions, thus allowing great advances when used as signal reporters (*e.g.*, avoiding background fluorescence, increasing photostability and improving signal-to-noise ratio and sensitivity in complex biological samples). However, LFAAs using UCNPs as fluorescence signal generators have not been reported yet.

In this study, we developed a novel LFAA for simultaneously detecting multiple types of targets (*i.e.*, bacteria, small molecules and ions). To improve the detection sensitivity, UCNPs with red, green and blue emission peaks were synthesized and used as detection probes generating fluorescence signal. However, the generation of fluorescence signal requires 980 nm laser irradiation and the fluorescence intensity should be further related to the targets concentrations. We therefore designed a portable reader to improve the usability of the assays, which allows us to simultaneously detect and quantify multiple targets using an LFAA and obtain the results *via* a smartphone. The conclusions can be drawn from the presence and level of each target from the presence and color intensity of a corresponding colored band. The developed LFAA enables sensitive and specific detection of multiple targets using different aptamers, which lends itself to potential applications in the monitoring of quality and safety for various foodstuffs.

2. Materials and methods

2.1. Materials

1-Ethyl-3-(3-dimethylaminopropyl)-carbodiimide hydrochloride (EDC), N-hydroxysulfosuccinimide sodium salt (sulfo-NHS), poly (acrylic acid) (PAA, Mw = 800–1000), $ErCl_3{\cdot}6H_2O$, $YCl_3{\cdot}6H_2O$, $TmCl_3{\cdot}6H_2O$, $YbCl_3{\cdot}6H_2O$ and NH_4F were all purchased from Sigma Aldrich. 1-Octadecene (90%) sodium and oleic acid (90%) were obtained from Alfa Aesar. NaOH, methanol, chloroform, ethanol, saline-sodium citrate (SSC), Tris-HCl, Tween 20 and bovine serum albumin (BSA) were obtained from Tianjin Zhiyuan Chemical Reagent Co., Ltd. Aptamers and their complementary sequences (Table 1) were selected according to literature [26–28] and synthesized by Shanghai General Biological Science & Technology Company.

Table 2
The dosage of rare-earth chlorides.

UCNPs	Dosage of rare-earth chlorides
$NaYF_4$:Yb,Er (Green)	$YCl_3{\cdot}6H_2O$ (242.69 mg, 0.8 mmol), $ErCl_3{\cdot}6H_2O$ (7.64 mg, 0.02 mmol) and $YbCl_3{\cdot}6H_2O$ (69.75 mg, 0.18 mmol)
$NaYF_4$:Yb,Tm (Blue)	$YCl_3{\cdot}6H_2O$ (210.8 mg, 0.695 mmol), $YbCl_3{\cdot}6H_2O$ (116.2 mg, 0.30 mmol), and $TmCl_3{\cdot}6H_2O$ (1.9 mg, 0.005 mmol).
$NaYF_4$: Er,Tm (Red)	$YCl_3{\cdot}6H_2O$ (267.0 mg, 0.88 mmol), $TmCl_3{\cdot}6H_2O$ (7.7 mg, 0.02 mmol), $ErCl_3{\cdot}6H_2O$ (38.2 mg, 0.1 mmol)
Enhanced $NaYF_4$: Er,Tm (Red)	$YCl_3{\cdot}6H_2O$ (267.0 mg, 0.88 mmol)

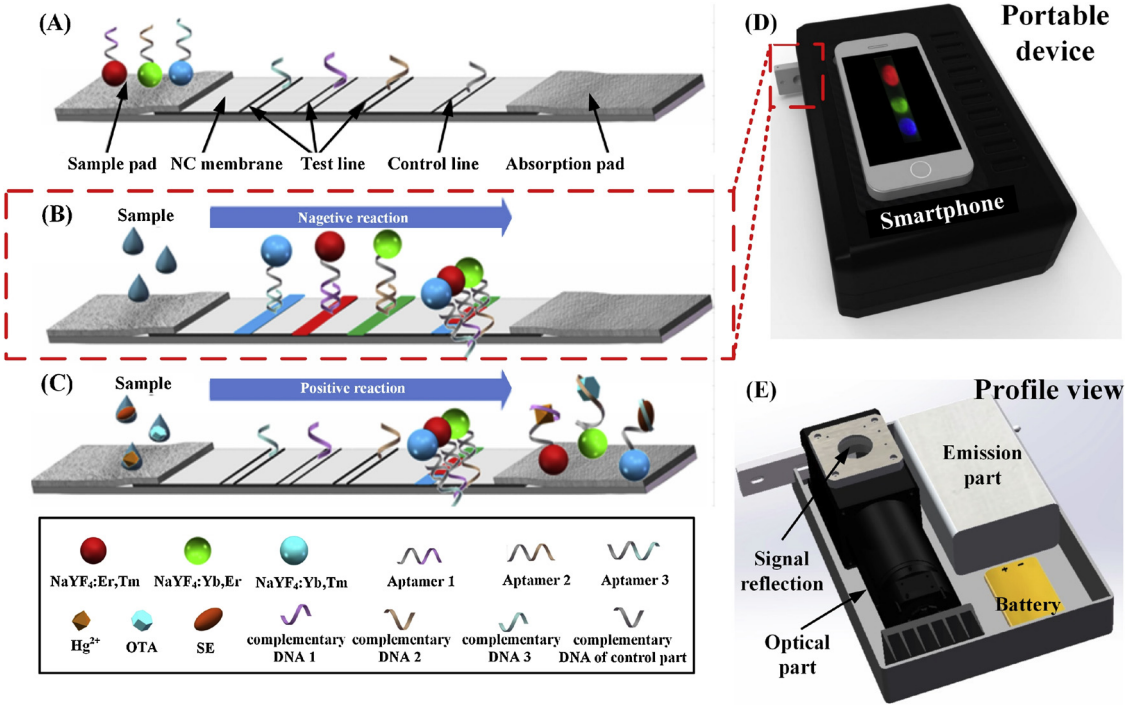

Fig. 1. Schematic illustration of LFAA for simultaneous multiple targets detection.
(A) The structure of the developed LFAA. The three kinds of ssDNA sequences were attached to three kinds of UCNPs (red, green and blue) by a condensation reaction, respectively. Streptavidin was used as an intermediate to react with both biotin and the NC membrane to immobilize complementary DNA of aptamer parts and control parts on an NC membrane. We mixed probes in buffer solution, this solution was further mixed with sample solution and was finally detect by the design strip. (B) In the absence of target, UCNP probes were separately hybridized with the corresponding complementary DNA. (C) In the presence of targets (*i.e.*, bacteria, small molecules and metal ions), the aptamers preferentially bonded to the corresponding targets and caused fewer aptamers hybridized with complementary DNA, thereby liberating UCNPs and resulting in fluorescence decrease. The color intensities of the corresponding test zones gradually decrease as the concentrations of the analytes in the samples increase. (D) A smartphone-based portable device is using to read the detection results. (E) The schematic of the smartphone-based portable device. (For interpretation of the references to colour in this figure legend, the reader is referred to the web version of this article.)

2.2. Synthesis and surface modification of UCNPs

UCNPs were synthesized according to the protocol from the literature [29]. For three types of UCNPs, rare-earth chlorides were mixed with a different molar ratio as shown in Table 2. The mixture was dissolved in water (2 mL) and then added to a flask containing 1-octadecene (30 mL) and oleic acid (12 mL). The oxygen was removed from the obtained mixture for 5 min. The mixture was then heated to 160 °C under the protection of argon atmosphere and keeping for 1 h to remove water. And then the solution was cooled down to room temperature. Then, NH_4F (148.15 mg, 4 mmol) and NaOH (100 mg, 2.5 mmol) were dissolved in 10 mL of a methanol and added into the flask. The mixture was then kept stirring for 2 h at room temperature. Next, the mixture was heated to 296 °C after methanol evaporation, and then maintained for 1.5 h before cooling down. The product was then centrifuged and washed with cyclohexane and ethanol for two times, respectively, and was finally stored in cyclohexane (10 mL).

Core-shell UCNPs with enhanced fluorescence intensity were synthesized following the protocol from the literature [4]. For formation of the shell, $YCl_3{\cdot}6H_2O$ (267.0 mg, 0.88 mmol) was added to a flask containing 1-octadecene (15 mL) and oleic acid (7.5 mL). The detailed process was the same as mentioned in the synthesis process of the core UCNPs. It is noteworthy that the core UCNPs (5 mL) with red emission should be added and then the mixture should be heated to 100 °C to remove cyclohexane.

The surface modification of UCNPs was achieved by a ligand exchange process [30]. PAA, as a multidentate ligand, was used to displace the original hydrophobic ligands on the UCNPs surface by mixing PAA (15.8 mg), UCNPs (1 mL), ethanol (2 mL) in chloroform (1 mL). The mixture was dispersed and stirring overnight. Then, the product was centrifuged and washed with ethanol for two times. Then the obtained product was re-dispersed in PBS (5 mL).

2.3. Attachment of aptamers to the UCNPs

UCNP-aptamer conjugates were prepared using the condensation reaction [17]. As-prepared UCNPs-PAA (500 μL) was centrifuged at 8000 rpm for 8 min and re-suspended in 500 μL of MES buffer (50 mM, pH = 6.1). EDC (2 mg/mL, 120 μL) and sulfo-NHS (2 mg/mL, 60 μL) were subsequently added into the mixture and kept standing for 2 h. The aptamer solution (2 nmol/mL, 400 μL) was added into the mixture and then overnight incubated. Then the aptamer conjugated UCNPs were centrifuged and washed for two times with Tris-HCl buffer and then finally re-dispersed in Tris-HCl buffer (500 μL). The red $NaYF_4$: Er, Tm nanoparticles (**rUCNP**) with aptamer 1 (for Hg^{2+}) is called **R-probe** hereinafter. And the green $NaYF_4$: Yb,Er (**gUCNP**) with aptamer 2 (for ochratoxin A) and blue $NaYF_4$: Yb,Tm (**bUCNP**) with aptamer 3 (for Salmonella) are called **G-probe** and **B-probe**, respectively.

2.4. Preparation of LFAA

The lateral flow aptamer assay was prepared following the protocol from the literature [31]. An absorbent pad (2.5 × 30 cm), a nitrocellulose membrane (NC membrane, 2.0 × 30 cm) and an immersing pad (1.9 × 30 cm) were pasted on a backing pad (6.0 × 30 cm) with 2 mm overlap between every two adjacent pads. Then the as-prepared pads were cut into strips with a width of 2.5 mm using Matrix 2360™ Programmable Shear. Control and test zones were separately generated by dispensing capture and control probe (100 μM, 0.3 μL).

Streptavidin was used as an intermediate to immobilize control and

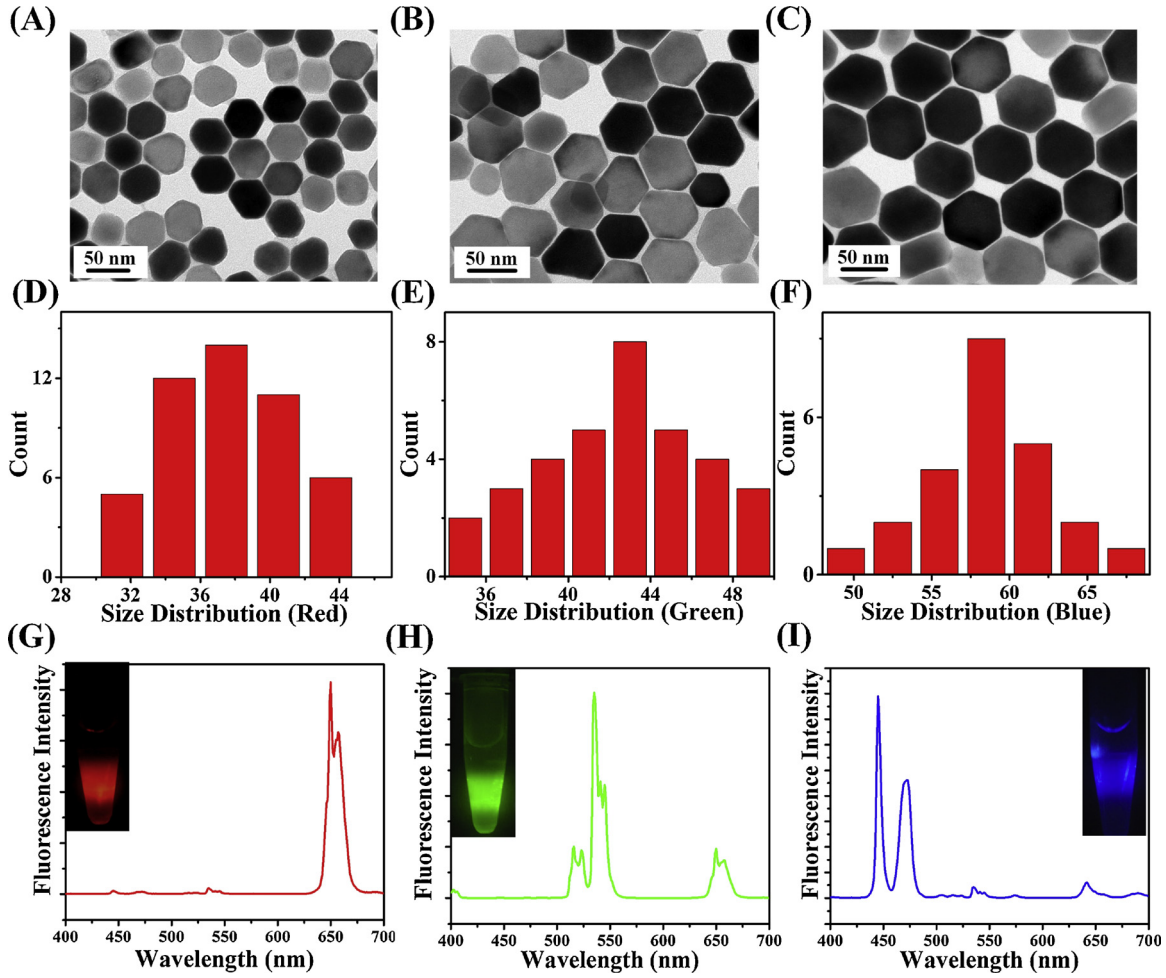

Fig. 2. Characterization of UCNPs.
TEM images of (A) $NaYF_4$: Er,Tm, (B) $NaYF_4$:Yb,Er and (C) $NaYF_4$: Yb,Tm. The size distribution of (D) $NaYF_4$: Er,Tm, (E) $NaYF_4$:Yb,Er and (F) $NaYF_4$:Yb,Tm. Fluorescence emission spectrum of (G) $NaYF_4$: Er,Tm, (H) $NaYF_4$:Yb,Er and (I) $NaYF_4$: Yb,Tm. Insets of (G–I) show photographs of the solution of $NaYF_4$: Er,Tm, $NaYF_4$:Yb,Er and $NaYF_4$: Yb,Tm excited by a 980 nm laser, respectively.

capture probes on the NC membrane due to that it can react with both biotin and the NC membrane. Briefly, complementary DNA of aptamers and control probes were previously biotinylated. For the control zone, control probe (6.27 nmol) was added into 62.7 μL of streptavidin (1 mg/mL). For the test zone, 34.2 μL, 28.8 μL, 66.7 μL of streptavidin (1 mg/mL) were added into bacteria, molecule and ions capture probe, respectively (dry powder, 3.42 nmol, 2.88 nmol, 6.67 nmol). The obtained probes were incubated at 25 °C for 40 min. The final concentration of each probe was 100 μM. Finally, the control and capture probes (0.3 μL) were added onto the NC membrane and dried in an oven at 37 °C for 2 h.

2.5. Sample preparation

For bacteria targets, bacteria strains used in this research were Salmonella (ATCC 50761), *E. coli* (ATCC 8739), *Staphylococcus aureus* (ATCC 25923) and *Bacillus subtilis* (ATCC 6633). Salmonella (SE) was selected as analyte for bacteria detection while other bacteria were selected as control groups. For a small molecule, ochratoxin A (OTA) was selected as a target while Aflatoxin B1, kanamycin and melamine were selected as control groups. For ion target, mercury ion was selected as target for ion detection while lead ion, cupric ion and ferrous ion were selected as control groups.

2.6. Detection of targets

Running buffer was prepared by adding SSC (2×), Tween 20 (0.5% v/v), BSA (4% w/v) into Tris-HCl (10 mM, pH 7.4) buffer. Then three UCNPs probes were added into running buffer as a ratio of R-probe: G-probe: B-probe: running buffer = 2 μL:0.2 μL:1.2 μL:20 μL. Subsequently, the as-prepared probe (20 μL) was pipetted separately into sample solution (60 μL). Immobilizing probes in immersion pad requires a large number of optimization processes (*e.g.* concentration and composition of buffer, concentration of probe, drying time) [32,33]. We therefore mixed probes in buffer solution rather than immobilizing probes in the immersion pad, which could make the experiment process more convenient and stabile. The LFAAs were submerged into the mixture for 30 min and then removed. We used the 980 nm laser to hit the assay at a 45-° position to excite the test zone. The camera (Nikon D90) was fixed to a tripod to upright against the assay and the exposure time was set to 4 s to obtain the strongest signal while avoiding overexposure. The quantitative detection of fluorescence intensities was performed by image processing with ImageJ to quantify the fluorescence intensities. We repeated 5 groups of detections to obtain the average values and standard deviation and evaluated the detection limit of the developed LFAA for each target. The quantitative results were also performed using a smartphone and a handhold device developed by our lab (see Fig. S7A for details).

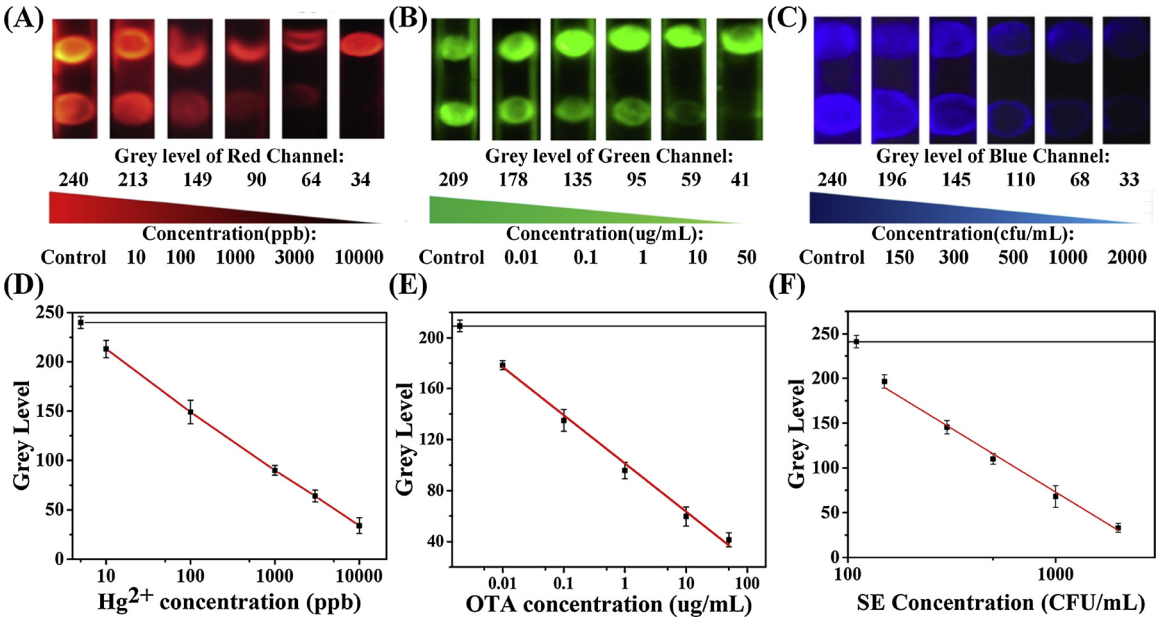

Fig. 3. Detection of a single target using the developed LFAA. (For interpretation of the references to colour in the text, the reader is referred to the web version of this article.)
The fluorescence images show the grey level decreases (A) with the increasing Hg^{2+} concentration, (B) with increasing OTA concentration, (C) with the increasing SE concentration. Standard curves of the relative grey level of (D) red channel *versus* Hg^{2+} concentration, (E) green channel *versus* OTA concentration and (F) blue channel *versus* Salmonella concentration show linear relationship. (For interpretation of the references to colour in this figure legend, the reader is referred to the web version of this article.)

3. Results and discussion

3.1. Design of the LFAA for multiple targets detection

The principles of the multiplex detection of bacteria, small molecules and metal ions using multicolor LFAA are schematically described in Fig. 1. Three kinds of amino-modified ssDNA sequences (Table 1) are attached to the three carboxyl-functionalized UCNPs with different emission colors, respectively, through a condensation reaction. Streptavidin is used as an intermediary to react with both biotin and the NC membrane. It will immobilize the complementary DNA of the aptamer and the control parts on the NC membrane. The operation of the developed LFAA is based on the competition between targets in the samples and the complementary DNA of the aptamer conjugates, which are immobilized on the NC membrane for binding to the multicolor UCNPs-labeled aptamers. Hence, the fluorescence intensity of the corresponding test zones gradually decreases as the concentration of the targets in the samples increases. The detection results could be read using a smartphone and a portable device (Fig. 1D). The schematic of the developed device is shown in Fig. 1E.

3.2. Characterization of UCNPs

Sensitive and stable target detection requires UCNPs to have good surface characteristics and high fluorescence intensity. A series of characterizations were conducted to assess the morphology, size and surface characteristics of the UCNPs. $NaYF_4$ was chosen as the host material for the UCNPs due to its high chemical stability and low phonon energies ($\sim 350\ cm^{-1}$). Various rare-earth chlorides were doped on the $NaYF_4$ to make three kinds of UCNPs with different emission peaks. The dosages are shown in Table 2. XRD patterns show all the diffraction peaks can be ascribed to the hexagonal structure of $NaYF_4$ (JCPDS no. 16-0334), which indicate that $NaYF_4$ exhibits a pure hexagonal phase (Fig. S1). We also checked the morphology of three kinds of UCNPs using transmission electron microscopy (TEM) and observed that rUCNPs, gUCNPs and bUCNPs all have hexagonal structures (Fig. 2A–C). From the elemental analysis, we observed that rUCNPs, gUCNPs and bUCNPs have an average diameter of 38 nm, 45 nm and 54 nm and the molarity of r-UCNPs, g-UCNPs and b-UCNPs are 39 nM, 24 nM and 14 nM, respectively (Fig. 2D–F, see Supporting Information for the calculation details). The successful modification of PAA on the UCNPs was confirmed by FT-IR spectroscopy (Fig. S2A), which can be further confirmed by the clear polymer layer observed on the surface of UCNPs from the HRTEM image (Fig. S2B). After re-dispersing the obtained UCNPs-PAA in ultrapure water and under 980-nm excitation, we observed red, green and blue emissions at peaks of 650 nm, 540 nm and 450 nm from rUCNPs, gUCNPs and bUCNPs, respectively (Fig. 2G–I). We also observed that, compared to gUCNPs and bUCNPs, rUCNPs show a weaker emission intensity, which may affect the reading of fluorescence intensity from different colors when using multiple target detection. This may because of the much larger 980 nm absorption of Yb^{3+} ($^2F_{7/2}\rightarrow{}^2F_{5/2}$) than that of Er^{3+} ($^4I_{11/2}\rightarrow{}^4I_{15/2}$) [32]. Therefore, core-shell structured rUCNPs ($NaYF_4$@$NaYF_4$:Er,Tm) with a concentration of 39 nM were used instead to enhance red fluorescence (Fig. S3).

We prepared the three conjugates, *i.e.*, core-shell rUCNPs-aptamer 1 (for Hg^{2+}), gUCNPs-aptamer 2 (for OTA) and bUCNPs-aptamer 3 (for SE), to detect the three different targets. The carboxyl groups on the surface of PAA-UCNPs were activated using sulfo-NHS and EDC, and the activated carboxyl groups were then reacted with the amine groups on the aptamers. The successful connection of aptamers and UCNPs was confirmed using UV–vis absorption spectroscopy. No absorption peak was observed *via* UV–vis spectroscopy in the UCNPs-PAA before conjugating with aptamers. However, an absorption peak at approximately 260 nm of the aptamer was detected after the conjugation reaction. (Fig. S4).

3.3. Optimization of the multiple target LFAA

The operation of the multiple target LFAA is based on the competition between targets in the sample and the complementary DNA of aptamers conjugated on the surface of the working membrane for

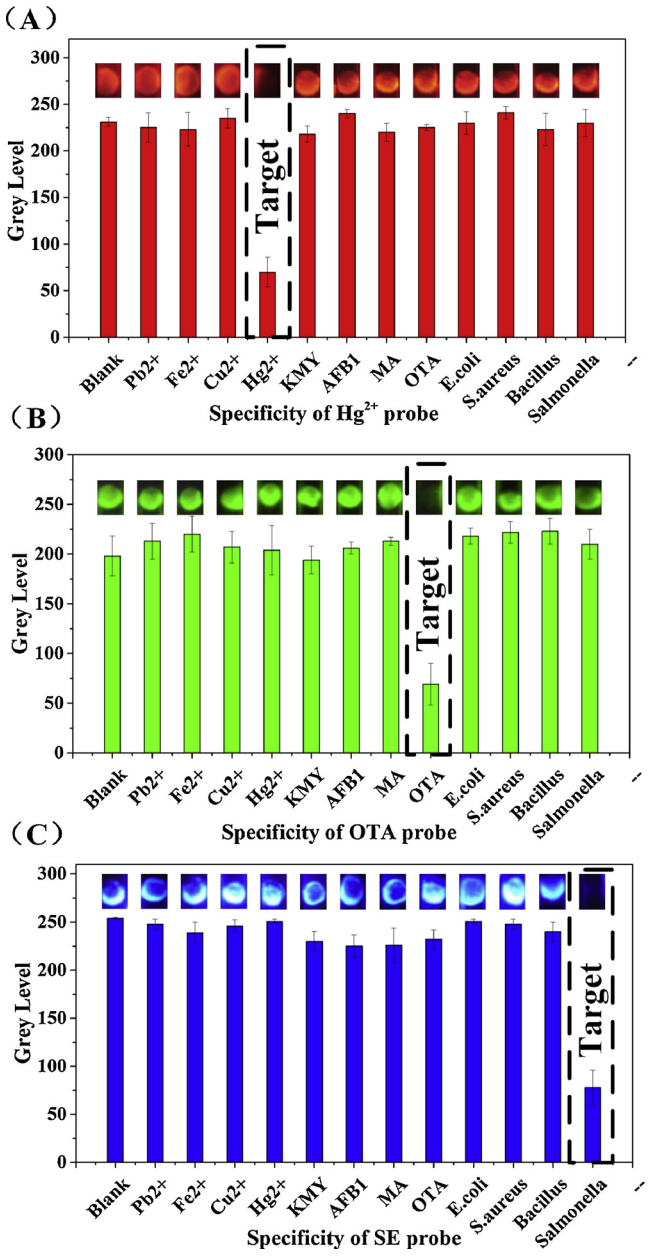

Fig. 4. Specificity evaluation of the developed LFAA.
Change in grey level with various types of targets (A) using R-probe, (B) using G-probe and (C) using B-probe. (Concentration was 10^3 CFU/mL, 10 μg/mL and 10^3 ppb for each bacteria, molecules and ions, respectively.)

binding to the UCNP-aptamer probes. Hence, the fluorescence intensity of the corresponding test zones gradually decreases as the analyte concentration increases.

The optimal composition (*e.g.*, running buffer and concentration of BSA, SSC and UCNP probes) of the detection system should provide the minimum detection limit as well as precise and quantitative detection of the targets. Through optimization, we obtained the final running buffer which contains Tris-HCl (10 mm, pH 7.4), tween 20 (0.5% v/v), BSA (4% v/w) and 2 × SSC. In addition, probe concentration can affect sensitivity and signal intensity. Probe concentrations (0.2 μL for G-probes (4.8 nM), 1.2 μL for B-probes (2.8 nM) and 2 μL for R-probes (8 nM)) were optimized to ensure both signal intensity and sensitivity. The detailed optimized process is shown in Figs. S5–S6.

3.4. Evaluation of the detection limit and specificity

We prepared single-target LFAAs using R-probes, G-probes and B-probes, and repeated 5 groups of experiment to evaluate the detection limit of the developed LFAA for different targets. (*e.g.*, OTA, Hg^{2+} and SE) (Fig. 3). We observed that the grey level of the test zone gradually decreases as the corresponding target concentration increases by examining the detected gradient concentration of the targets (Fig. 3A–C). To quantitative analysis the results, we use ImageJ to select the test zone and estimate the average grey level. The selection of test zone was shown as Fig S7A, a circle tool was used to framing the test zone along the border. The target concentrations are proportional to the decrease in the grey level of test zone, implying a linear relationship in the detection range of 10–10^4 ppb for Hg^{2+}, 0.01–50 μg/mL for OTA and 150–2000 CFU/mL for SE (Fig. 3D–F). Statistical analysis reveals that the detection limit reaches 5 ppb, 3 ng/mL and 85 CFU/mL for Hg^{2+}, OTA and SE, respectively, which were calculated by the ratio of three times of the standard deviation of the blank signals. Target detection can be completed within 30 min using the developed LFAA without the need for enrichment using the developed LFAA, which is significantly faster than the traditional methods, such as PCR [33], ELISA [34], colony culture and counting [35] and the electrochemical method [36]. In addition, the auto-fluorescence of some targets (*e.g.*, bacteria and biotoxin) can be avoided because UCNPs are excited by 980 nm NIR radiation. The detection sensitivity can be significantly improved as compared with gold nanoparticles or traditional fluorescence materials. For instance, the detection limit for OTA is 10 ng/mL [37], and for Salmonella is 10^4 CFU/mL [38] both using gold nanoparticle based lateral flow assay. The lateral flow assay using quantum dots for foodborne pathogen can improve the detection limit to 3000 CFU/mL [39], which highlights its potential use for sensitive POCT.

We added other targets (*e.g.*, *E. coli*, *Bacillus subtilis*, *Staphylococcus aureus*, Aflatoxin B1, kanamycin, melamine, lead ions, cupric ions and ferrous ions) into the sample to test the specificity of the developed LFAA (Fig. 4). In the example shown in Fig. 4A, we analyzed the grey level of the test zone by adding all the targets to the above R-probe and observed that only Hg^{2+} induced a dramatic fluorescence decrease at the corresponding grey level channel. We further quantified the grey level for different targets and found that Pb^{2+}, Cu^{2+}, Fe^{2+} and other molecules and bacteria in this system had negligible effects on the test zone. These results demonstrate that the R-probe exhibits good specificity. In the same way, we also prove that these control targets have no significant effect on the G-probe and B-probe (Fig. 4B–C).

3.5. Integration for multiple targets detection

After proving the sensitivity and specificity of the developed single-target LFAA was satisfactory, we proceeded to assess our LFAA for multiple target testing. To this end, we integrated three test zones into one assay and added analytes to prove that the developed LFAA could detect three targets simultaneously. It's noteworthy that we proved that the LFAA was working. Therefore, in the case of multiple detection, we removed the control zone. As shown in Fig. 5A, three test zones (red, green and blue) can be observed in the absence of three analytes (control experiment) and the corresponding test zone eventually disappears upon adding each analyte. We compared the detection results from multiple targets and single-target detection. And the result in Fig. 5B shows that there is no significant difference between the two, indicating that the developed LFAA is capable of multiple targets detection. It is known that the potential disadvantages of multiplexing include non-specific binding and crossover reaction, leading to false positive results. An increase in the number of analytes may cause serious crossover reaction. This difficulty in distinguishing between simultaneously detected analytes can be overcome by using multicolor signals on a single test strip [14]. The advantages of using multicolor probes over single-color probe modified with different aptamers lie in:

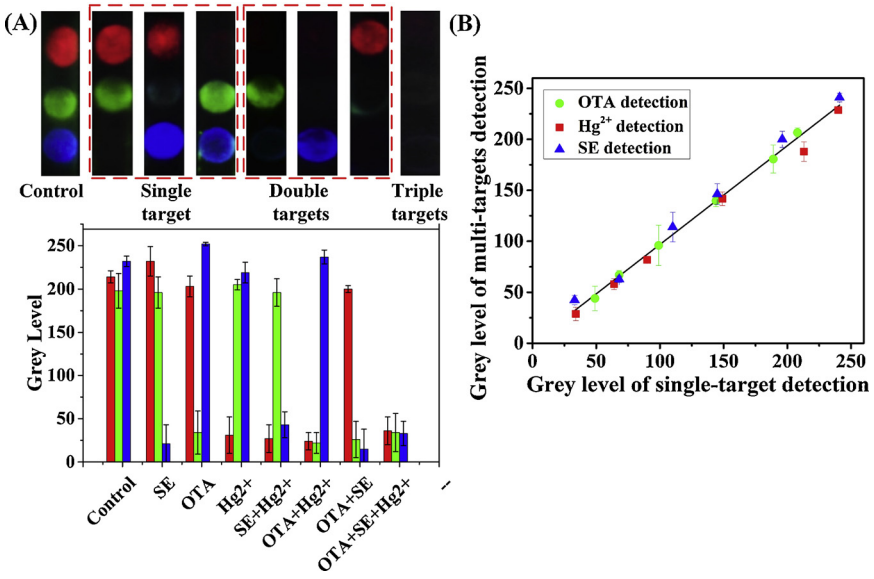

Fig. 5. Multiplex detection of three targets using multiple targets LFAA.
(A) The complementary DNA of each target aptamer were added on individual detection areas. A mixture of R-probe, G-probe, and B-probe was in the conjugate pad. When no targets are detected, the corresponding UCNPs probe forms three colored bands at the specific line. When the infectious targets are detected, the grey level of corresponding test zones decrease. The below is a quantitative analysis of grey level. (Concentration was 10^4 CFU/mL, 100 μg/mL and 10^4 ppb for each bacteria, molecules and ions, respectively). (B) Linear correlation between the multiple targets detection and single-target detection. (For interpretation of the references to colour in the text, the reader is referred to the web version of this article.)

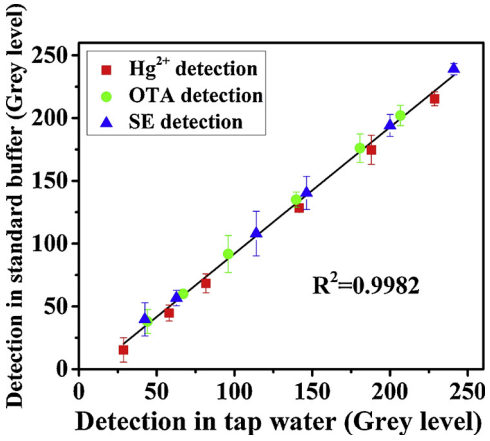

Fig. 6. Correlation between the detection results in the real sample (tap water) and running buffer.

The crossover reaction could be obviously observed by using of multicolor probes, in which case single-color probe is not working; (ii) We measured the results by splitting color area to RGB channels, which are exactly correspond to the colors of three UCNPs probes. Thus by using multicolor probes, we can still analyze the results when crossover reaction occurred (Fig. S7B). Thus, the developed LFAA addresses the issue of crossover reaction from different analytes as involved in the traditional methods. On the other hand, unlike traditional multiplex LFAs, which can only detect the same type of target, the developed LFAA is able to detect different kinds of targets owning to the use of aptamers.

The accuracy and practical application of the developed LFAA was evaluated using tap water as a real sample because the targets hereinbefore may all appear in water. The samples were spiked with OTA, Hg^{2+} and SE at different concentrations without pretreatment. The entire detection process was completed in about 30 min, and the results are shown in Fig. 6. We observed that the analyzed results using tap water were generally less than results in the running buffer, which is probably because the concentration of BSA, SSC were lower in the system. However, the analyzed trend still maintains a good linear relationship. Thus, we can still obtain accurate results using a correction factor. The performance in this application clearly demonstrates that the developed LFAA can efficiently detect and quantify multiple targets in real samples.

To further demonstrate the application of our LFAA for POCT, we read the results using a smartphone-based reader developed by our lab to make the detection process more portable (Fig. S8A) [4]. As shown in Fig. S8B, the grey level of the results from our developed platform is lower than the results from the CCD camera. This may be because the exposure of the smartphone is not as good as the CCD camera. However, the results still maintain a good linear relationship. This result indicates that the developed LFAA can be used in resource-limited settings *via* such smartphone-based reader. In addition, the manufacturing cost can be greatly reduced due to the application of the paper-based structure and aptamer. Unlike traditional detection methods that require large devices and expensive supplies to meet detection requirements (*e.g.*, sensitive, specific, multiple targets), our developed LFAA is able to sensitively and rapidly detect multiple targets with a portable device and low-cost supplies.

4. Conclusions

In this study, we developed a lateral flow aptamer assay integrated smartphone-based portable device to achieve specific and sensitive detection of multiple targets with different analyte-recognition reactions (*e.g.*, ochratoxin A, mercury ions and Salmonella) simultaneously. The detection limits for mercury ions, ochratoxin A and *Salmonella* are 5 ppb, 3 ng/mL and 85 CFU/mL, respectively. The use of upconversion nanoparticles with different emission bands as the core of the detection probes avoids the problem of crossover reactions from different analytes enabling an efficient method for multiple target detection. We also demonstrate that the aptamer-based recognition method provides unprecedented advantages for the detection of multiple targets with different analyte-recognition reactions in a single lateral flow strip. The detection platform was tested successfully in the detection of ochratoxin A, mercury ions and Salmonella in real water samples (*i.e.*, tap water) within 30 min. Therefore, the developed detection platform offers a novel approach for sensitive, specific, convenient detections, which holds enormous potential for detecting a wide range of targets in water and food samples.

Acknowledgements

The work was financially supported by the Natural Science Basic Research Plan in Shaanxi Province of China (2017KJXX-28), the Fundamental Research Funds for the Central Universities (2016qngz), National Instrumentation Program (2013YQ190467), the Natural

Science Foundation of China (81601553), Key Program for Science and Technology Innovative Research Team in Shaanxi Province of China (2017KCT-22) and Program for Innovative Research Team in Yulin, Shaanxi Province of China (2017KJJH-02).

Appendix A. Supplementary data

Supplementary material related to this article can be found, in the online version, at doi:https://doi.org/10.1016/j.snb.2018.08.074.

References

[1] X. Zhang, Z. Dai, S. Si, X. Zhang, W. Wu, H. Deng, et al., Ultrasensitive SERS substrate integrated with uniform subnanometer scale “hot spots” created by a graphene spacer for the detection of mercury ions, Small 13 (2017).
[2] J. Zhang, Y.-K. Xia, M. Chen, D.-Z. Wu, S.-X. Cai, M.-M. Liu, et al., A fluorescent aptasensor based on DNA-scaffolded silver nanoclusters coupling with Zn (II)-ion signal-enhancement for simultaneous detection of OTA and AFB 1, Sens. Actuators B: Chem. 235 (2016) 79–85.
[3] Z.A.I. Mazrad, I. In, K.-D. Lee, S.Y. Park, Rapid fluorometric bacteria detection assay and photothermal effect by fluorescent polymer of coated surfaces and aqueous state, Biosens. Bioelectron. 89 (2017) 1026–1033.
[4] M. You, M. Lin, Y. Gong, S. Wang, A. Li, L. Ji, et al., Household fluorescent lateral flow strip platform for sensitive and quantitative prognosisof heart failure using dual-color upconversion nanoparticles, ACS Nano 11 (2017) 6261–6270.
[5] F. Chaib, WHO’s First Ever Global Estimates of Foodborne Diseases Find Children Under 5 Account for Almost One Third of Deaths, (2015).
[6] Y. Dong, Y. Xu, W. Yong, X. Chu, D. Wang, Aptamer and its potential applications for food safety, Crit. Rev. Food Sci. Nutr. 54 (2014) 1548–1561.
[7] L. Zhan, S.Z. Guo, F. Song, Y. Gong, F. Xu, D.R. Boulware, et al., The role of nanoparticle design in determining analytical performance of lateral flow immunoassays, Nano Lett. 17 (2017) 7207–7212.
[8] L. Blanco-Covián, V. Montes-García, A. Girard, M.T. Fernández-Abedul, J. Pérez-Juste, I. Pastoriza-Santos, et al., Au@ Ag SERRS tags coupled to a lateral flow immunoassay for the sensitive detection of pneumolysin, Nanoscale 9 (2017) 2051–2058.
[9] V.C. Ozalp, D. Cam, F.J. Hernandez, L.I. Hernandez, T. Schafer, H.A. Oktem, Small molecule detection by lateral flow strips via aptamer-gated silica nanoprobes, Analyst 141 (2016) 2595–2599.
[10] A.N. Berlina, N.A. Taranova, A.V. Zherdev, Y.Y. Vengerov, B.B. Dzantiev, Quantum dot-based lateral flow immunoassay for detection of chloramphenicol in milk, Anal. Bioanal. Chem. 405 (2013) 4997–5000.
[11] S. Song, N. Liu, Z. Zhao, E. Njumbe Ediage, S. Wu, C. Sun, et al., Multiplex lateral flow immunoassay for mycotoxin determination, Anal. Chem. 86 (2014) 4995–5001.
[12] Y. Xu, Y. Liu, Y. Wu, X. Xia, Y. Liao, Q. Li, Fluorescent probe-based lateral flow assay for multiplex nucleic acid detection, Anal. Chem. 86 (2014) 5611–5614.
[13] C.W. Yen, H. de Puig, J.O. Tam, J. Gomez-Marquez, I. Bosch, K. Hamad-Schifferli, et al., Multicolored silver nanoparticles for multiplexed disease diagnostics: distinguishing dengue, yellow fever, and Ebola viruses, Lab Chip 15 (2015) 1638–1641.
[14] N.A. Taranova, A.N. Berlina, A.V. Zherdev, B.B. Dzantiev, ‘Traffic light’ immunochromatographic test based on multicolor quantum dots for the simultaneous detection of several antibiotics in milk, Biosens. Bioelectron. 63 (2015) 255–261.
[15] M.-Z. Zhang, M.-Z. Wang, Z.-L. Chen, J.-H. Fang, M.-M. Fang, J. Liu, et al., Development of a colloidal gold-based lateral-flow immunoassay for the rapid simultaneous detection of clenbuterol and ractopamine in swine urine, Anal. Bioanal. Chem. 395 (2009) 2591–2599.
[16] X. Ren, A.D. Gelinas, I. von Carlowitz, N. Janjic, A.M. Pyle, Structural basis for IL-1alpha recognition by a modified DNA aptamer that specifically inhibits IL-1alpha signaling, Nat. Commun. 8 (2017) 810.
[17] B. Jin, S. Wang, M. Lin, Y. Jin, S. Zhang, X. Cui, et al., Upconversion nanoparticles based FRET aptasensor for rapid and ultrasenstive bacteria detection, Biosens. Bioelectron. 90 (2017) 525–533.
[18] N. Mohammad Danesh, M. Ramezani, A. Sarreshtehdar Emrani, K. Abnous, S.M. Taghdisi, A novel electrochemical aptasensor based on arch-shape structure of aptamer-complimentary strand conjugate and exonuclease I for sensitive detection of streptomycin, Biosens. Bioelectron. 75 (2016) 123–128.
[19] A. Abbaspour, F. Norouz-Sarvestani, A. Noori, N. Soltani, Aptamer-conjugated silver nanoparticles for electrochemical dual-aptamer-based sandwich detection of staphylococcus aureus, Biosens. Bioelectron. 68 (2015) 149–155.
[20] Y. Wu, S. Zhan, H. Xing, L. He, L. Xu, P. Zhou, Nanoparticles assembled by aptamers and crystal violet for arsenic(III) detection in aqueous solution based on a resonance Rayleigh scattering spectral assay, Nanoscale 4 (2012) 6841–6849.
[21] A. Dhiman, P. Kalra, V. Bansal, J.G. Bruno, T.K. Sharma, Aptamer-based point-of-care diagnostic platforms, Sens. Actuators B: Chem. 246 (2017) 535–553.
[22] N.H.A. Raston, V.-T. Nguyen, M.B. Gu, A new lateral flow strip assay (LFSA) using a pair of aptamers for the detection of Vaspin, Biosens. Bioelectron. 93 (2017) 21–25.
[23] M. Jauset-Rubio, Mt. Svobodová, T. Mairal, C. McNeil, N. Keegan, M.S. El-Shahawi, et al., Aptamer lateral flow assays for ultrasensitive detection of β-conglutin combining recombinase polymerase amplification and tailed primers, Anal. Chem. 88 (2016) 10701–10709.
[24] G. Shen, S. Zhang, X. Hu, Signal enhancement in a lateral flow immunoassay based on dual gold nanoparticle conjugates, Clin. Biochem. 46 (2013) 1734–1738.
[25] J. Liu, D. Mazumdar, Y. Lu, A simple and sensitive “dipstick” test in serum based on lateral flow separation of aptamer-linked nanostructures, Angew. Chem. 118 (2006) 8123–8127.
[26] J.A. Cruz-Aguado, G. Penner, Determination of ochratoxin a with a DNA aptamer, J. Agric. Food Chem. 56 (2008) 10456–10461.
[27] X. Ma, Y. Jiang, F. Jia, Y. Yu, J. Chen, Z. Wang, An aptamer-based electrochemical biosensor for the detection of Salmonella, J. Microbiol. Methods 98 (2014) 94–98.
[28] Q. Li, M. Michaelis, G. Wei, L. Colombi Ciacchi, A novel aptasensor based on single-molecule force spectroscopy for highly sensitive detection of mercury ions, Analyst 140 (2015) 5243–5250.
[29] M. You, M. Lin, S. Wang, X. Wang, G. Zhang, Y. Hong, et al., Three-dimensional quick response code based on inkjet printing of upconversion fluorescent nanoparticles for drug anti-counterfeiting, Nanoscale 8 (2016) 10096–10104.
[30] B. Jin, M. Lin, M. You, Y. Zong, M. Wan, F. Xu, et al., Microbubble embedded with upconversion nanoparticles as a bimodal contrast agent for fluorescence and ultrasound imaging, Nanotechnology 26 (2015) 345601.
[31] J. Hu, L. Wang, F. Li, Y.L. Han, M. Lin, T.J. Lu, et al., Oligonucleotide-linked gold nanoparticle aggregates for enhanced sensitivity in lateral flow assays, Lab Chip 13 (2013) 2285–2288.
[32] H. Dong, L.-D. Sun, C.-H. Yan, Energy transfer in lanthanide upconversion studies for extended optical applications, Chem. Soc. Rev. 44 (2015) 1608–1634.
[33] E. Morales-Narvaez, T. Naghdi, E. Zor, A. Merkoci, Photoluminescent lateral-flow immunoassay revealed by graphene oxide: highly sensitive paper-based pathogen detection, Anal. Chem. 87 (2015) 8573–8577.
[34] C.-M. Shih, C.-L. Chang, M.-Y. Hsu, J.-Y. Lin, C.-M. Kuan, H.-K. Wang, et al., Paper-based ELISA to rapidly detect Escherichia coli, Talanta 145 (2015) 2–5.
[35] K. Tsougeni, G. Papadakis, M. Gianneli, A. Grammoustianou, V. Constantoudis, B. Dupuy, et al., Plasma nanotextured polymeric lab-on-a-chip for highly efficient bacteria capture and lysis, Lab Chip 16 (2016) 120–131.
[36] Y. Lian, F. He, H. Wang, F. Tong, A new aptamer/graphene interdigitated gold electrode piezoelectric sensor for rapid and specific detection of Staphylococcus aureus, Biosens. Bioelectron. 65C (2014) 314–319.
[37] J. Moon, G. Kim, S. Lee, Development of nanogold-based lateral flow immunoassay for the detection of ochratoxin A in buffer systems, J. Nanosci. Nanotechnol. 13 (2013) 7245–7249.
[38] C.C. Liu, C.Y. Yeung, P.H. Chen, M.K. Yeh, S.Y. Hou, Salmonella detection using 16S ribosomal DNA/RNA probe-gold nanoparticles and lateral flow immunoassay, Food Chem. 141 (2013) 2526–2532.
[39] J.G. Bruno, Application of DNA aptamers and quantum dots to lateral flow test strips for detection of foodborne pathogens with improved sensitivity versus colloidal gold, Pathogens 3 (2014) 341–355.

Birui Jin was born in P.R. China. He received his B.E. degree in Thermal & Power Engineering and Industry Engineering and M.E. degree in Materials Science and Engineering from Xi’an Jiaotong University, and now is pursuing the Ph.D. degree of Materials Science and Engineering in Xi’an Jiaotong University. His work focuses on studying the upconversion-aptamer probes for POC detection.

Yang Yexin was born in P.R. China. She received the B.E. degree from China Medical University, Shenyang, China in 2016, and now is pursuing the master degree of School of Life Science and Technolegy in Xi’an Jiaotong University, Shaanxi, China. Her work focuses on μPADs(Microfluidic Paper-based Analytical Devices).

Rongyan He was born in P.R. China. She received the B.E. degree from Xi’an Jiaotong University of Life Science and Technology in 2016, and now is pursuing the Ph.D. degress in Xi’an Jiaotong University. Her work focuses on point-of-care test and long-term monitoring.

Yong Il Park was born in Republic of Korea. He received the B.S. and Ph.D degree in Chemical and Biological Engineering from Seoul National University. He was then appointed assistant professor at school of chemical engineering, Chonnam National University. His work focuses on biomedical application and energy application.

Aeju Lee was born in Republic of Korea. She was then appointed assistant professor at International Research Organization for Advanced Science and Technology (IROAST), Kumamoto University. Her works focuses on nanoimaging sensor, drug delivery and nanomedicine.

Dan Bai was born in P.R. China. She received B.S. degree in Applied Chemistry from both Xi’an Shiyou University and Troy University, followed by acquiring M.S. degree in Drug Chemistry and Ph.D. degree in Molecule Photonics from Newcastle University. She was then appointed lecturer at School of Medicine, Xi’an Jiaotong University. Dr. Bai’s current research is focused on (i) Aptamer based point-of-care testing (POCT); (ii) Theranostic agents.

Fei Li was born in P.R. China, and obtained her B.Sc. in Chemistry from Northwestern University (China), M.Sc. in Analytical Chemistry from Changchun Institute of Applied Chemistry of Chinese Academy of Sciences (China) in 2004, and Ph.D. in Chemistry from University of Warwick (U.K.) in 2008, respectively. During 2008–2010, she worked as postdoctoral fellow at Ecole Polytechnique Federale de Lausanne (Switzerland) and Temple University (U.S.A.). Since 2011, Dr. Li joined at Xi’an Jiaotong University (China) as an associate professor. Her current research is focused on studying cell behaviors in

three-dimensional microenvironment using electrochemical scanning probe microscopy techniques and developing paper-based point-of-care platforms.

Tian Jian Lu was born in P.R. China. He received the B.S. and M.E. degrees in Applied Mechanics from Xi'an Jiaotong University, and the Ph.D. in Engineering Sciences from Harvard University. Before joining Xi'an Jiaotong University in 2004 as a full professor in Applied Mechanics, Dr. Lu was a Lecturer, Reader and Professor in Materials Engineering at Cambridge University. Dr. Lu's main interest in bioengineering is fundamental and applied research concerning highly porous materials and their applications, including bio-heat transfer, bio-mechanics and 3D cell microenvironment.

Feng Xu was born in P.R. China. He received his B.S. in both Thermal & Power Engineering and Industry Engineering and M.S. in Mechanical Engineering from Xi'an Jiaotong University, and his Ph.D. in Engineering from Cambridge University. He worked as a research fellow at Harvard Medical School and Harvard-MIT Health Science & Technology (HST). Currently, Dr. Xu is a full professor at School of Life Science and Technology, Xi'an Jiaotong University. Dr. Xu's current research focuses on Bio-thermo-mechanics, Engineering of Cell Microenvironment, and Point-of-Care Technologies.

Min Lin was born in P.R. China. He achieved B.S. degree in Material Science and Engineering from Hefei University of Technology and M.S. degree in Material Science and Engineering from Xi'an Jiaotong University. Dr. Lin completed his Ph.D. degree at Bioinspired Engineering and Biomechanics Center in Xi'an Jiaotong University. He joined the faculty of Xi'an Jiaotong University in 2011 and was promoted as an Associate Professor in 2016. During 2014–2015, Dr. Lin worked as a research fellow at Harvard Medical School and Massachusetts General Hospital. Dr. Lin's current research is focused on biomaterials/nanomaterials synthesis (*e.g.*, upconversion nanoparticles) and biomedical applications such as gene/drug delivery and point-of-care diagnosis.